

Distinctive Patterns of Dominant Frequency Trajectory Behaviour in Persistent Atrial Fibrillation: Spatio-temporal Characterisation

JL Salinet¹, J Tuan², ASM Salinet¹, X Li¹, P Stafford², GA Ng¹⁻³, FS Schlindwein^{1,3}

¹Departments of Engineering and Cardiovascular Sciences, University of Leicester, UK

²University Hospitals of Leicester NHS Trust, UK

³NIHR Leicester Cardiovascular Biomedical Research Unit, Glenfield Hospital, UK

Abstract

Enhancing our understanding of the underlying AF behaviour is a key factor to contribute towards improving patient outcomes in special for persistent AF (persAF) patients. In this study different signal processing and visualisation techniques were developed and applied to simultaneous high density sets of intracardiac electrograms (EGMs) obtained from persAF. We demonstrated that DF of EGMs lacked in spatiotemporal stability, hence targeting sites of peak DF from a single time frame is unlikely to be a reliable ablation strategy. Tracking the centre of gravity (CGs) from the highest dominant frequency areas (HDFAs) revealed three distinct propagation behaviours favouring the cyclical and local activity. The cores of the HDFAs showed to be significantly more organised than their periphery. Real-time implementation was shown to be feasible with the use of Graphic Processing Units representing an innovation that is currently being considered as part of the decision to guide ablation therapy for persAF.

1. Introduction

Atrial fibrillation (AF) is the commonest heart rhythm disturbance in clinical practice [1]. Its symptoms and morbidity are responsible for frequent medical appointments and admissions imposing great strain on healthcare resources [2]. AF presence, especially in long-term, promotes pronounced electrical and structural atrial substrate remodelling and enlargement with fibrosis contributing to its recurrence (AF begets AF) [3, 4].

Although research groups are dedicating extensive investigations to understanding the physiopathology of AF, some of the mechanisms of triggering and maintenance of this arrhythmia are still unrevealed. Moreover, there are controversies regarding the most acceptable theories [5, 6]. The multiple-circuit re-entry, together with the refinement of Moe's theory and the observation of the maximum number of simultaneous re-

entry circuits have been the dominant conceptual AF model until recently. However, it has been strongly challenged by a series of studies showing evidences that (1) AF was primarily triggered by rapidly firing foci originated on the pulmonary veins (PVs) [1]; and (2) excitable spiral waves propagating around an unexcited core, identified as 'rotors', were found as uninterrupted periodic activity associated to the highest dominant frequencies (DF) [7]. Additionally, preferable inter-atrial pathways with evidence of fibrillatory conduction associated with the presence of frequency gradients between left atrium (LA) and right atrium were also observed [7].

This phenomenon was later evidenced by clinical studies conducted in humans AF showing that targeting sites of highest DF may be important for catheter ablation [8, 9]. It had also been demonstrated that ablation reduces the DF of AF electrograms [10] and that a decrease in DF may be associated with a more favourable outcome [8]. However, DF-guided ablation has not been widely adopted and published data using this approach is limited, partly because its clinical significance is not fully understood.

This study aimed to characterise the spatiotemporal behaviour of relevant DF areas including characteristics of the highest DF area (HDFA) and its organisation during AF using non-contact mapping (NCM) in patients with persistent AF (persAF) to help further understand the significance and utility of real-time DF mapping.

2. Methods

2.1. Electrophysiology study

A non-contact multi-electrode array (MEA) catheter (EnSite 3000, St Jude Medical, USA) was introduced trans-septally into the LA of eight patients (age: 47±10 years; AF duration: 34±25 months) undergoing catheter ablation of persAF for the first time and with no previous history of heart diseases. Without contact between the

endocardium wall and electrodes from the MEA [11], the system generates reconstructed unipolar virtual electrograms (EGMs) using inverse solution mathematics [12] projected to the endocardial 3D geometry of the LA. Anatomical landmarks were identified and annotated on the detailed endocardial 3D LA surface.

To avoid isopotential map distortion the MEA was not moved after geometry creation [11, 12] and the distance between the centre of the MEA and the LA endocardial wall did not exceed 4 cm. After EGMs acquisition in AF steady state, the MEA was removed and AF ablation proceeded as per standard practice. This study had informed consent from the patients undergoing persAF ablation for the use of electrical data acquired.

2.2. Signal processing

For each patient, high density mapping with 2048 simultaneous EGMs during longer AF episodes (> 1 minute) were exported and analysed off-line using Matlab (MathWorks Inc., USA). EGMs were sampled at 1200 Hz and high-pass filtered at 1 Hz. No further filtering was applied to the signals to preserve signal integrity and low frequency components [13].

To avoid hampering the AF behaviour analysis and the possibility of distorted results, an effective far-field cancellation method is of importance prior conducting further analysis in AF. QRS-T removal was implemented by a recently validated technique using individually 'customized' and adaptive QRS-T segmentation and a coherent subtraction strategy [14].

After carrying out ventricular cancellation, spectral analysis was performed for each of the 2048 EGMs, using Fast Fourier Transform (FFT) with a Hamming window to produce 3D DF maps [15]. A window size of 4 s was chosen and sequential windows were obtained with 50% overlap (shifting forward by 2 s) over a period of 1 minute to produce sequential frequency maps for each patient. The spectral resolution was 0.25 Hz and fivefold zero padding was applied (frequency step of 0.05 Hz). DF was defined as the frequency with highest power within the physiological relevant range from 4 Hz to 10 Hz [15]. In addition, organization index (OI) was computed as an auxiliary parameter to measure spectral organisation and/or signal quality [16]. The higher the OI value the more 'organised' the DF electrogram is:

$$OI = \frac{\text{Area}(DF+\text{harmonics})}{\text{Whole AF spectrum area}}, \quad (1)$$

2.3. Spatiotemporal DF analysis

For the purpose of assessing temporal stability of DF, we compared the DF of all EGMs between consecutive time windows (at 2 s intervals), to investigate if the DF

remained within a defined threshold of ± 0.25 Hz or ± 0.50 Hz [15]. If the DF wandered beyond the pre-defined threshold over time, the frequency value was deemed 'unstable'. After identifying that DF was not consistently stable over time, further analysis on DF behaviour was performed to investigate if DF values show any temporal repetition or spatial 'reappearance', so as to quantify the presence of any potential DF partial 'periodicity'. This was done by using the first DF value from each point of interest as a reference, which was then compared with the DF values from the same location while moving forward 2 s in time (Figure 1). The proportion of DF points falling within the thresholds of ± 0.25 or ± 0.50 Hz compared to their corresponding reference DF value were plotted over time and defined as DF reappearance points. The time (in seconds) corresponding to any partial 'periodicity' or 'reappearance' of the overall DF behaviour was assessed and called 'DF reappearance interval'.

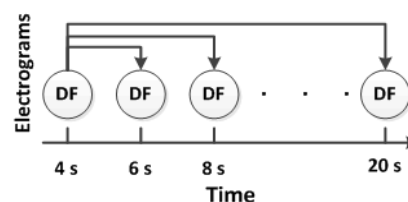


Figure 1. Illustration of the method used for DF reappearance analysis.

Associated with the analysis from the 3D DF maps previously described and for further investigation, areas with highest dominant frequency (HDFA) on the 3D DF maps were isolated for each time segment, together with its neighbouring sites, which contained DF values within 0.25 Hz of the highest DF [15]. This produced an area consisting of a collection of points that reflect average regional activity, to minimise the effect of isolated high DF sites. The centre of gravity (CG) for the HDFAs was identified by averaging the coordinate positions of each point in the cloud, weighted by their respective DF values [15]. These CG points were obtained for each 4 s FFT window and tracked at 2 s intervals over the entire period, so as to produce a HDFA trajectory map. It was followed by investigating the relationship of electrograms' DF organisation of sites localised on the HDFAs core (OI_{CG}) and sites of HDFAs encountered on the cloud boundary or periphery (OI_{Per}).

3. Results

A total of 232 sequential DF maps were analysed. Sequential analysis of individual AEGs of longer segments and global DF maps revealed a general lack of temporal DF stability throughout, although periods of apparent stability were also observed. Approximately 60% of the EGMs of all patients lost stability in the first 2

s (0.25 Hz threshold) and 40% (0.5 Hz threshold). Individual analysis of EGMs also revealed episodes suggestive of repetition or reappearance of DF over time, where DF loses temporal stability, only to return to a value very close to that of the initial DF (see Figure 2). DF reappearance interval from the population was 8.0 ± 2.4 s (0.25 Hz) and 9.8 ± 6.5 s (0.5 Hz threshold).

Having seen the dynamic DF behaviour, the analysis proceeded with the tracking of HDFAs at each time point by plotting the trajectory of its CG, so as to determine its spatial-temporal characteristics. This revealed 3 global patterns of behaviour (Figure 3): Type I (Local activity) – CG propagation trajectory area < 5% of the LA area over consecutive time frames; Type II (Cyclical) – CG propagation trajectory area > 5% of LA area but showing a trajectory that returns to the vicinity of at least one of its earlier CG sites over time; Type III (Irregular) – CG propagation trajectory area > 5% of LA area with a non-cyclical pattern of movement and no overlap of CGs over consecutive time frames.

A total of 7 local activity events (mean time per event: 2.86 ± 1.07 s), 15 cyclical events (5.07 ± 1.49 s), and 2 irregular events (4.50 ± 1.91 s) were identified over analysis of 20 s-long segments from all patients. When the analysis to 1 minute was extended, the number of events increased respectively to 24, 54 and 6. The mean times spent in each separate event were similar between 20 s and 1 minute analyses (2.86 ± 1.07 s vs. 2.83 ± 1.55 s, $p = 0.9701$ for local activity; 5.07 ± 1.49 s vs. 5.14 ± 2.16 s, $p = 0.2620$ for cyclic activity; and 4.5 ± 1.91 s vs. 4.60 ± 0.97 s, $p = 0.29$ for irregular activity). Cyclical activity was the most prevalent behaviour observed (61.2 ± 12.4 % of the time), followed by local (27.0 ± 8.6 %) and then irregular activity (11.9 ± 9.1 %). All except one patient had cyclical activity as the predominant behaviour over 20 s and 1 minute. The DF trajectory showed a concentration of HDFAs on the roof and around the PVs. The mean HDFA value was 7.29 ± 0.71 Hz.

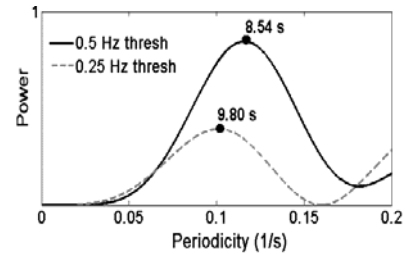
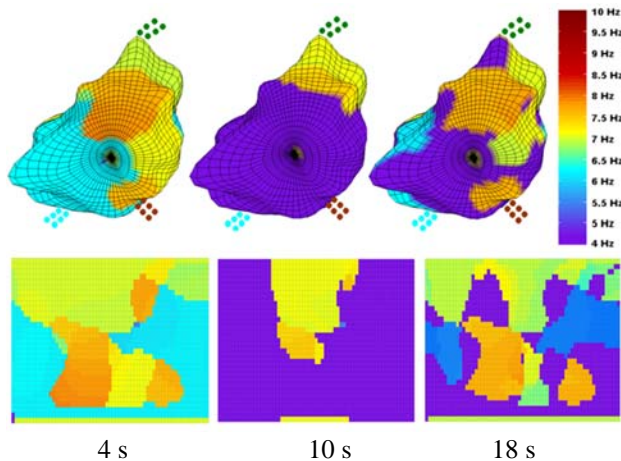


Figure 2. DF map showing DF reappearance projected onto its 3D LA geometry. Its respective 2D map is also displayed. Sites containing the higher DF values (in yellow and orange) at 4 s, no longer do so at 10 s, but reappear partially at 18 s (orange areas). The respective periodicity of DF reappearance for both thresholds is also presented.

The electrograms' DF organisation of the HDFAs at the CG core (OI_{CG}) was compared with sites located on the periphery (OI_{Per}) and a typical example is presented in Figure 4. When the analysis was expanded to the entire population, sites with highest DF had a greater degree of organisation at their core (CG) compared to their periphery: 0.43 ± 0.17 and 0.36 ± 0.10 respectively ($p = 0.0061$).

Finally, the processing time of sequential 3D DF frames showed feasible for real-time applications. It decreased from 2.46 ± 0.05 s (single core) to 2.03 ± 0.03 s (four cores) and 0.27 ± 0.01 s (480 GPU cores).

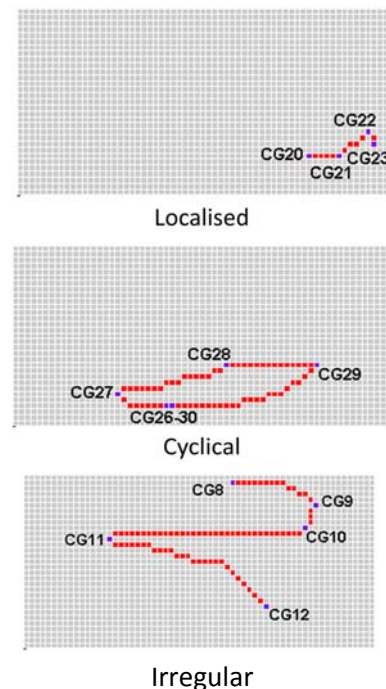


Figure 3. The 3 types of trajectory behaviour seen on the persAF patients: type 1 - Localised, type 2 - Cyclical and type 3 - Irregular.

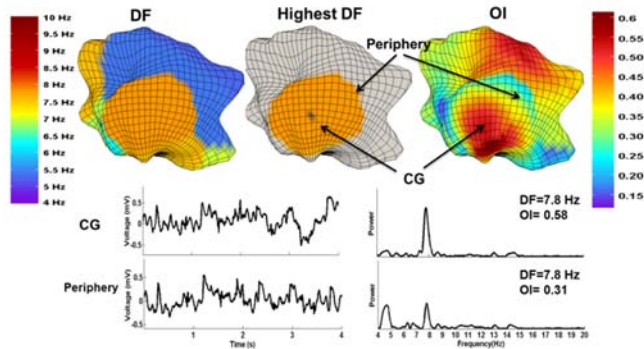


Figure 4 – A typical example showing the HDFA with a greater degree of organisation at the core (CG) compared to its periphery.

4. Discussion and conclusions

Using high density NCM of the LA, we have demonstrated that DF of EGMs lack in spatiotemporal stability. Hence targeting sites of peak DF from a single time frame is unlikely to be a reliable ablation strategy. Tracking of the CGs of the HDFAs revealed the presence of localised, cyclical and irregular patterns of propagation where the cores of the HDFAs were found to be significantly more organised than their periphery. In these areas (core), there were fast and organized activity and, when moving to the HDFAs' periphery the DF organisation reduced significantly (multiple peaks at the electrograms' spectrum) maybe due wavefront collisions.

We observed a predominance of local and cyclical maximal DF activity. This may imply in a higher proportion of rotor driven episodes, although the lack of spatiotemporal DF stability makes it unlikely that AF is being primarily sustained by anatomically stationary high DF sites. The presence of a cyclical pattern does suggest a certain extent of spatial consistency. Irregular maximal DF propagation was seen in our study, and it would be analogous to multiple wavelet activity. It is of note that in our study all 3 patterns of behaviour were observed in the same individual patient over time. In addition, it is likely that more than one mechanism may be involved in AF perpetuation at different stages of the arrhythmia history in any given individual. Depending on the extent of electromechanical remodelling and autonomic influence, a particular mechanism may predominate, resulting in different subtypes of persAF. This could explain why an anatomical-based ablation strategy tends to produce only modest results for persAF. A tailored ablation approach should therefore be considered for each individual case, provided that effective real-time, high resolution DF mapping can be performed. Currently, a 3D DF mapping GUI platform has been created with the analysis present on this study embedded including the HDFAs trajectory tool to guide catheter ablation in persAF patients. The clinical outcomes are currently being assessed.

References

- [1] Haïssaguerre M, Jais P, Shah DC, Takahashi A, Hocini M, Quiniou G, Garrigue S, Le Mouroux A, Le Metayer P, Clément J. Spontaneous initiation of AF by ectopic beats originating in the PVs. *New Engl J Med* 1998;339:659-66.
- [2] Fuster V, Ryden LE, Cannom DS, Crijns HJ, Curtis AB, Ellenbogen KA, Halperin JL *et al.*. ACC/AHA/ESC Guidelines for the management of patients with AF-executive summary. *Circulation* 2006;114:700-752.
- [3] Crandall MA, Bradley DJ, Packer DL, Asirvatham SJ. Contemporary management of AF: update on anticoagulation and invasive management strategies. *Mayo Clin Proc* 2009;84:643-662.
- [4] Kirchhof P, Eckardt L. Ablation of AF: for whom and how? *Heart* 2010;96:1325-1330.
- [5] Nattel S., Ehrlich JR. Atrial fibrillation. In: ZipesDP, Jalife J, editors. In: *Cardiac Electrophysiology From Cell To Bedside* 2004. Philadelphia: Saunders.
- [6] Prystowsky EN. The history of AF: the last 100 years. *J Cardiovasc Electr* 2008;19:575-582.
- [7] Jalife J, Berenfeld O, Mansour M. Mother rotors and fibrillatory conduction: a mechanism of AF. *Cardiovasc Res* 2002;54:204-216.
- [8] Yoshida K, Chugh A, Good E, Crawford T, Myles J, Veerareddy S, Billakanty S, *et al.*. A critical decrease in DF and clinical outcome after catheter ablation of persistent AF. *Heart Rhythm* 2010;7:295-302.
- [9] Atienza F, Almendral J, Jalife J, *et al.*. Real-time dominant frequency mapping and ablation of DF sites in AF with left-to-right frequency gradients predicts long-term maintenance of SR. *Heart Rhythm* 2009; 6:33-40.
- [10] Takahashi Y, Sanders P, Jais P, Hocini M, Dubois R, Rotter M, Rostock T, Nalliah CJ, Sacher F, Clémenty J, Haïssaguerre M: Organization of frequency spectra of AF: relevance to radiofrequency catheter ablation. *J Cardiovasc Electr* 2006; 17:382-388.
- [11] Chinitz LA, Sethi JS. How to perform noncontact mapping. *Heart Rhythm* 2006;3:120-123.
- [12] Schilling RJ, Peters NS, Davies W. Simultaneous endocardial mapping in the human LV using a noncontact catheter - Comparison of contact and reconstructed electrograms during SR. *Circulation* 1998;98:887-898.
- [13] Gojraty S, Lavi N, Valles E, Kim SJ, Michele J, Gerstenfeld EP. Dominant frequency mapping of AF: comparison of contact and noncontact approaches. *J Cardiovasc Electr* 2009;20:997-1004.
- [14] Salinet Jr JL, Madeiro JPV, Cortez PC, Stafford PC, Ng GA, Schlindwein FS. Analysis of QRS-T subtraction in unipolar AF electrograms. *Med Biol Eng Comput* 2013;51:1381-91.
- [15] Salinet JL, Tuan JH, Sandilands AJ, Stafford PJ, Schlindwein FS, Ng GA. Distinctive patterns of DF trajectory behavior in drug-refractory persistent AF: Preliminary characterization of spatio-temporal instability. *J Cardiovasc Electr* 2014; 25:371-379.
- [16] Everett TH, Kok LC, Vaughn RH, Moorman JR, Haines DE. Frequency Domain algorithm for quantifying AF organization to increase defibrillation efficacy. *IEEE Trans on Biomedical Engineering* 2001;48:969-978.

Address for correspondence:

João Salinet, University of Leicester (joasalinet@hotmail.com)